*Mon. Not. R. astr. Soc.* (1980) **192**, 53–74

# Optical polarization of the Seyfert galaxies MRK 3, MRK 231, NGC 3227 and NGC 3516

Ian Thompson* and J. D. Landstreet* *Department of Astronomy, University of Western Ontario, London, Ontario N6A 5B9, Canada*

H. S. Stockman and J. R. P. Angel *Steward Observatory, University of Arizona, Tucson, Arizona 85721, USA*

E. A. Beaver *Department of Physics, University of California at San Diego, La Jolla, California 92093, USA*

Received 1979 November 6; in original form 1979 July 26

**Summary.** Intermediate resolution observations of the emission line and continuum polarization of the Seyfert galaxies Mrk 3, Mrk 231, NGC 3227 and NGC 3516 are presented. For each galaxy, the polarization shows a strong wavelength dependence with the polarization increasing smoothly into the blue. This wavelength dependence, together with the presence of polarized Hα emission, argues strongly that the polarization of each galaxy is caused by an asymmetric dust envelope surrounding the nucleus. Observations of the polarization of the [O III] λ 5007 emission in Mrk 3 and NGC 3227 and the polarization through the non-stellar Na I *D* line absorption in Mrk 231 are used to place constraints on the extent of the polarizing clouds in these galaxies. No polarization variability was detected with time-bases ranging from a few weeks to three years.

## 1 Introduction

Initially, observations of optical polarization in active extragalactic objects were taken as evidence for non-thermal emission. Recent observations of the flat wavelength dependence of the polarization of Optically Violent Variables (OVV's) and BL Lacertae objects (Rudnick *et al.* 1978; Tapia *et al.* 1977; Rieke *et al.* 1977) together with the rapid variations in polarization and position angle (Angel *et al.* 1978) are still seen as evidence for direct non-thermal radiation. Similar behaviour is seen in the Seyfert galaxy NGC 1275 (Martin, Angel & Maza 1976).

However, observations of the continuum and emission line polarization in some Seyfert galaxies suggest that dust scattering processes are also important in producing the polarization. Permitted emission line polarization is the same as continuum polarization in NGC 1068 (Angel *et al.* 1976) and in Mrk 376 and IC 4329A (Stockman, Angel & Beaver 1976),

* Visiting astronomers, Kitt Peak National Observatory, which is operated by the Association of Universities for Research in Astronomy, Inc., under contract with the National Science Foundation.

showing that the observed nuclear polarization is produced *outside* the emission line region. Continuum circular polarization is seen in NGC 1068 (Angel *et al.* 1976), consistent with the polarization arising in thick dust clouds. Thompson *et al.* (1979) show that in NGC 4151, where the emission lines are unpolarized, the continuum polarization rises smoothly into the blue when corrected for the effects of hydrogen recombination radiation. A similar situation exists in Mrk 486 (Stockman 1979), suggesting the possibility that the polarization is produced by scattering in these two galaxies as well.

During the course of a programme to observe the wavelength dependence of the optical polarization of some bright Seyfert galaxies, we have observed the emission line and continuum polarization of the Seyfert galaxies Mrk 3, Mrk 231, NGC 3227 and NGC 3516. The polarization properties of all these galaxies resemble those of NGC 1068, suggesting that dust scattering is an important polarizer in all. In this paper, we present our polarimetric data on these galaxies and discuss qualitative models of them as suggested by the available data.

In Sections 2 and 3 we describe the details of the observations and the contributions from galactic interstellar polarization. In Sections 4 and 5 we present the polarization of the emission lines and continua of the observed galaxies. Finally, in Section 6 we discuss the results for each galaxy in terms of possible polarization mechanisms and current models for the nuclei of Seyfert galaxies.

**Table 1.**

| Filter | Wavelength (A) | Name |
|---|---|---|
| $CuSO_4$ + Hoya U330 | 3200 - 3850 | λ3500 |
| Interference | 4040 - 4800 | λ4400 |
| Corning 4-96 | 3800 - 5600 | λ4600 |
| Interference | 5550 - 6230 | λ5900 |
| Interference | 7100 - 7950 | λ7500 |
| Hoya IR80 | 8000 - 8600 | λ8300 |

## 2 Observations

Observations have been made with three different instruments: the University of Western Ontario (UWO) filter polarimeter, the Oke multichannel spectrophotometer (MCSP) and the University of California at San Diego (UCSD) Digicon detector.

Filter observations were obtained using the UWO two channel photoelectric Pockels cell polarimeter (Angel & Landstreet 1970a, b; Poeckert 1975) with the Kitt Peak National Observatory 1.3-m and 2.1-m telescopes and with the UWO 1.2-m telescope. The continuum observations of the four galaxies were made in bandpasses defined by commercial glass filters or interference filters together with the response of the RCA 31034A photomultipliers in the polarimeter. Table 1 lists the continuum filters used, their halfpower wavelengths and their designations as used in the rest of this paper. The continuum regions were chosen to avoid the strong emission lines of Hα; [N II] λλ 6548, 6584; Hβ; and [O III] λλ 4959, 5007. The line observations were made with interference filters with FWHP of 30 Å for the [O III] λ 5007 line and 35 Å for Hα. In general, line and continuum observations were obtained at the same time with roughly the same observing aperture. Bad weather prevented this for NGC 3516, for which no line observations were obtained with the UWO polarimeter, and for

Mrk 3. The line observations of Mrk 3 were obtained 1 to 2 months after the continuum observations with a further observation of Hα being made 1 yr later. Essentially simultaneous observations with the λ 5900 filter were made to check on possible continuum variations. No observations were made of Mrk 3 with the λ 3500 filter.

Observations of Mrk 231 and NGC 3516 were also made with the MCSP on the Hale Observatories 5.1-m telescope. The MCSP was adapted as a polarimeter as described by Angel & Landstreet (1974). The resolution was 160 Å below 5740 Å and 360 Å above. Rough spectrophotometry (± 0.2 mag) is available from the polarimetric data (Landstreet & Angel 1977). The standard star used was the white dwarf Grw + 70°8247 (Oke 1974).

Observations of Mrk 231 and NGC 3227 were obtained with the UCSD Digicon (Beaver *et al.* 1976) on the Steward Observatory 2.3-m telescope. The Digicon was attached to a flint prism spectrograph with a Pockels cell polarizing modulator. The data were smoothed with a

**Table 2.** Observations.

| Galaxy | Date (U.T.) | Instrument | Wavelength | Telescope | Aperture |
|---|---|---|---|---|---|
| Mrk 3 | 1976 Nov.17 | UWO | λ4400,λ5900 | UWO 1.2m | 7.7 |
| 2 | 1977 Mar 17 | UWO | λ7500 | UWO 1.2m | 7.7 |
| | 1977 Mar 19 | UWO | λ5900 | UWO 1.2m | 7.7 |
| | 1978 Feb 04 | UWO | λ4400, λ5900 | KP 2.1m | 4.6 |
| | | | λ7500, λ8300 | | |
| | 1978 Mar 09 | UWO | [O III] λ5007 | UWO 1.2m | 9.3 |
| | 1978 Mar 10 | UWO | λ5900 | UWO 1.2m | 9.3 |
| | 1978 Apr 09 | UWO | λ5900, Hα | UWO 1.2m | 7.7 |
| | 1979 Mar 23 | UWO | λ5900, Hα | UWO 1.2m | 7.7 |
| Mrk 231 | 1975 Apr 30 | MCSP | continuum, Hα | P 5.1 m | 3.6 |
| 1 | 1975 May 09 | Digicon | continuum, Hα | S 2.3m | 2.5 |
| | | | Fe II, Na I | | |
| | 1977 May 19 | UWO | λ4400,λ5900,λ7500 | KP 1.3m | 5.2 |
| | 1977 May 20 | UWO | λ3500 | KP 2.1m | 6.0 |
| | 1977 May 21 | UWO | λ8300, Hα | KP 2.1m | 6.0 |
| NGC 3227 | 1975 Apr 19 | Digicon | continuum, Hα, | | |
| 2 | | | [O III] λ5007,Hβ | S 2.3m | 2.5 |
| | 1977 May 15 | UWO | λ3500 | KP 1.3m | 5.2 |
| | 1977 May 22 | UWO | λ4400,λ5900, | KP 2.1m | 4.6 |
| | | | λ7500,λ8300 | | |
| | 1977 May 23 | UWO | [O III]λ5007,Hα | KP 2.1m | 6.0 |
| NGC 3516 | 1975 Apr 30 | MCSP | continuum, Hα | P 5.1m | 3.6 |
| 1 | 1978 Feb 04 | UWO | λ4600,λ5900, | KP 2.1m | 4.6 |
| | | | λ7500,λ8300 | | |

five substep (¼ diode) running mean. Due to the prism dispersion, the resolution varies from ≃ 15 Å at 4000 Å to ≃ 125 Å at 7000 Å.

A journal of the observations is given in Table 2. The table lists the galaxy observed and its Seyfert type (Weedman 1978), the UT data of the observation, the instrument, the wavelength range or filter, the telescope used and the diameter of the observing aperture. The designations of the filters used in the observations with the UWO polarimeter are from Table 1.

Each observation involved measuring the normalized Stokes parameters $Q = P\cos 2\theta$ and $U = P\sin 2\theta$, where $P$ is the polarization and $\theta$ the equatorial position angle. Observations have been corrected for instrumental efficiency and night sky background. Observations of interstellar polarization and null standards (Serkowski 1974) were used to establish instrumental efficiency, to reduce the position angle to the standard equatorial system, and to check for instrumental polarization.

Errors in the polarization are from counting statistics. We define the polarization $P$ by $P = \sqrt{(Q^2 + U^2 - \sigma_p^2)}$, where $\sigma_p$ is the assigned error in the polarization. The UWO and MCSP observations were made so that $\sigma_Q \simeq \sigma_U$ and $\sigma_p$ was taken to be $(\sigma_Q + \sigma_U)/2$. The error in position angle is $\sigma_\theta = 28^\circ.65\ \sigma_p/P$ for $\sigma_p < P$ and $52^\circ.0$ otherwise. The Digicon observations of Mrk 231, and to a lesser extent NGC 3227, were made such that more time was spent observing the $Q$ parameter and as a result $\sigma_Q < \sigma_U$. In these cases the errors $\sigma_p$ and $\sigma_\theta$ were weighted by the values of $Q$ and $U$ with

$$\sigma_p = \frac{\sqrt{[(Q\sigma_Q)^2 + (U\sigma_U)^2]}}{Q^2 + U^2}$$

and

$$\sigma_\theta = 28^\circ.65\frac{\sqrt{[(Q\sigma_U)^2 + (U\sigma_Q)^2]}}{Q^2 + U^2}.$$

Systematic errors of up to 2° are possible in the Digicon position angles.

The observed polarizations and position angles are shown in Figs 1–4. The error bars are $\pm\sigma_p$ and $\pm\sigma_\theta$. The data in some adjacent channels of the MSCP observations of Mrk 231 and NGC 3516 have been averaged in order to increase the signal-to-noise ratio. Representative spectrophotometry for the UWO observations of Mrk 3, Mrk 231 and NGC 3227 is taken from deBruyn & Sargent (1978) while the spectrophotometry for the MCSP observations of Mrk 231 and NGC 3516 is from the polarimetric data. In each case, $m_v = -2.5\log f_v + \text{constant}$. The upper panels in the figures showing the Digicon data of Mrk 231 and NGC 3227 display the total counts smoothed as for the polarimetric data.

We must consider the effects of aperture size on our observations of Mrk 3. Direct photographs with an Hα + [N II] filter show the emission to be extended over a region of ~ 10 arcsec (Weedman 1973) while Neugebauer *et al.* (1976) measure an increase by a factor of 1.2 in the Hβ flux in a 10 arcsec diaphragm compared to a 7 arcsec diaphragm. Balick & Heckman (1979) show that ~ 90 per cent of the [O III] λ 5007 flux is contained within a 6 arcsec aperture. Observations with the UWO polarimeter show that, within observing errors, all of the line flux is contained within a 7.7 arcsec diaphragm. Observations by Neugebauer *et al.* also show that the $V$ magnitude of Mrk 3 increases by 0.4 mag while an extrapolation of Weedman's (1973) multiaperture photometry shows an increase of 0.2 mag, both from 7 to 10 arcsec. These observations suggest that there could be polarization differences between the 4.6 and 9.3 arcsec apertures used in this study. No significant decrease in the polarization in the λ 5900 filter was found between these apertures (4.6

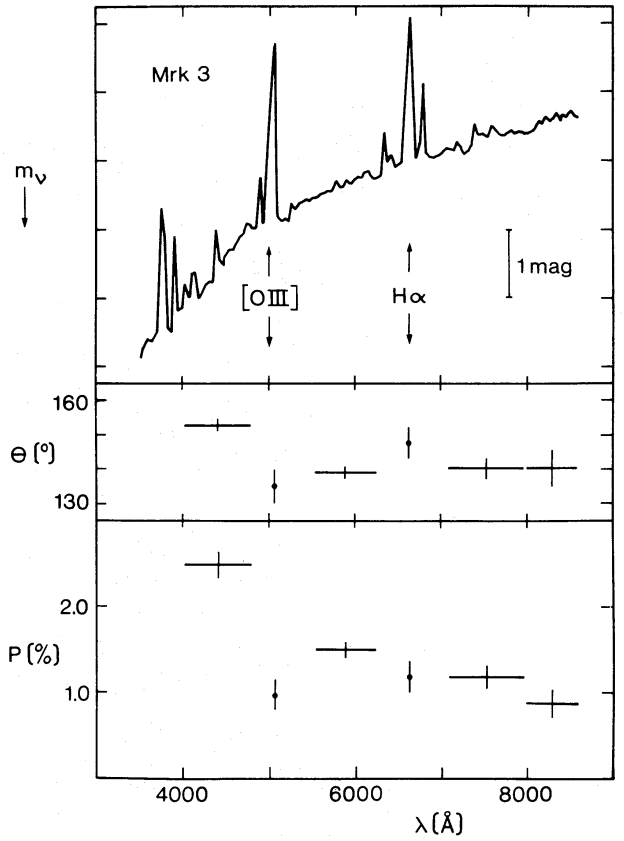


**Figure 1.** UWO polarimeter observations of Mrk 3. The spectrophotometry is from de Bruyn & Sargent (1978).

arcsec: $P = 1.65 \pm 0.12$ per cent, $\theta = 139°.0 \pm 2.0$; 9.3 arcsec: $P = 1.45 \pm 0.19$ per cent, $\theta = 140°.4 \pm 3°.8$). In addition, as discussed in Section 5.3, no variability is indicated by any of our observations of this galaxy. As a result, a weighted mean has been taken of all of the available data for each filter and these means have been plotted in Fig. 1.

Aperture effects are not important for the other galaxies, either because all the observations for a particular galaxy were made with approximately the same aperture size or because the apertures used were small enough to allow the Seyfert nucleus to dominate.

## 3 Galactic interstellar polarization

Three of the galaxies (Mrk 231, NGC 3227 and 3516) are at high galactic latitude ($b^{II} > 42°$) and so contributions to the observed polarization from aligned dust grains in our own Galaxy are expected to be low ($P \lesssim 0.2$ per cent). However, the galactic latitude of Mrk 3 is only $+22°.5$. In addition, the polarization of NGC 3516 is small enough that even a minor interstellar polarization could significantly affect the observed polarization spectrum. For these reasons a series of distant stars which are close to the galaxies on the sky were observed in the λλ 4400 and 5900 filters to determine the interstellar polarization in the direction of each galaxy. The stars were selected from the SAO catalogue to have $m_V$ fainter than 8.4, spectral types A2 or earlier, and galaxy–star separations of less than 3° on the sky.

The first three columns of Table 3 list the galaxies observed with their galactic latitude, and the polarization and position angles observed for each galaxy in the λλ 4400 and 5900 filters. The following columns give the stars near each galaxy which were observed for interstellar polarization, the values of $m_V$ and spectral type as given in the SAO catalogue, the

**Table 3.** Interstellar polarization observations.

| Galaxy $b^{II}$ | P(%) θ(°) λ4400 | P(%) θ(°) λ5900 | Star | $m_v$ Sp.type | $\Delta_r$ (arc min) | P(%) θ(°) λ4400 | P(%) θ(°) λ5900 |
|---|---|---|---|---|---|---|---|
| Mrk 3 | 2.45±0.15 | 1.49±0.08 | SAO 5821 | 8.5 | 32 | 0.110± 0.033 | 0.092± 0.032 |
| 22.5 | 152.0 ±1.8 | 139.3 ±1.5 | | A0 | | 179.9 ± 8.6 | 164.6 ±10.0 |
| | | | SAO 5813[1] | 9.0 | 61 | 0.862± 0.033 | 0.869± 0.036 |
| | | | | A0 | | 5.0 ± 1.1 | 4.3 ± 1.1 |
| | | | SAO 5738[2] | 8.5 | 93 | 0.032± 0.032 | 0.019± 0.034 |
| | | | | A0 | | 76.2 ±52.0 | 42.8 ±52.0 |
| | | | SAO 5658 | 9.0 | 138 | 0.263± 0.030 | 0.240± 0.036 |
| | | | | A0 | | 151.5 ± 3.3 | 148.3 ± 4.3 |
| | | | SAO 13742 | 8.9 | 180 | 0.081± 0.029 | 0.084± 0.035 |
| | | | | A2 | | 155.6 ±10.2 | 0.9 ±11.9 |
| | | | SAO 5838 | 8.8 | 109 | 0.037± 0.026 | 0.045± 0.032 |
| | | | | A0 | | 41.2 ±20.0 | 57.8 ±20.2 |
| | | | SAO 5784 | 9.1 | 151 | 0.379± 0.041 | 0.442± 0.048 |
| | | | | A0 | | 175.8 ± 3.1 | 171.1 ± 3.1 |
| Mrk 231 | 6.18±0.16 | 2.89±0.15 | SAO 28550 | 9.0 | 34 | 0.149± 0.054 | 0.124± 0.062 |
| 60.5 | 92.3 ±0.7 | 95.7 ±1.5 | | A0 | | 178.5 ± 9.1 | 0.4 ±12.8 |
| | | | SAO 28560 | 8.4 | 47 | 0.086± 0.029 | 0.0 ± 0.031 |
| | | | | | | 31.8 ± 9.6 | 25.8 ±52.0 |
| NGC 3227 | 2.16±0.10 | 0.97±0.10 | #2[3] | 11.1 | 11 | 0.053± 0.032 | 0.074± 0.039 |
| 55.5 | 131.2 ±1.4 | 137.4 ±2.8 | | | | 81.5 ±14.8 | 39.1 ±13.3 |
| | | | SAO 99114 | 8.9 | 46 | 0.051± 0.038 | 0.022± 0.037 |
| | | | | A2 | | 77.8 ±21.3 | 53.8 ±52.0 |
| NGC 3516 | 0.95±0.16 | 0.65±0.09 | SAO 7156 | 8.4 | 172 | 0.043± 0.031 | 0.019± 0.031 |
| 42.5 | 5.9 ±4.9 | 178.0 ±3.9 | | A2 | | 70.2 ±20.5 | 27.5 ±52.0 |
| | | | SAO 7270 | 8.8 | 36 | 0.244± 0.042 | 0.176± 0.037 |
| | | | | A2 | | 35.6 ± 4.9 | 21.8 ± 6.0 |
| | | | SAO 7273 | 9.0 | 110 | 0.0 ± 0.034 | 0.032± 0.037 |
| | | | | A0 | | 122.9 ±52.0 | 54.6 ±52.0 |
| | | | SAO 7409[4] | 9.2 | 144 | 0.053± 0.032 | 0.074± 0.039 |
| | | | | A0 | | 81.5 ±14.8 | 39.1 ±13.3 |

Notes to Table 3

1. Sanders A.J. 71, 719 — Star 624 70#8 V=8.24, B-V=0.02, U-B=-0.07
2. " — Star 624 70#2 V=8.51, B-V=0.16, U-B=0.15
3. Penston et al., PASP 83, 783 1971 — Star #4(NGC 3227) V=11.1, B-V=0.49, U-B=-0.10
4. Sanders A.J. 71, 719 — Star 1100 75#4 V=9.22, B-V=0.08, U-B=0.05

galaxy—star separation on the sky and the polarization and position angle in the λλ 4400 and 5900 filters.

As expected, polarization of the stars near Mrk 231 and NGC 3227 was not detected at the $3\sigma$ level. For Mrk 3, some of the observed stars show detectable polarization. There is no definite trend of polarization or position angle with either the star's magnitude or its position on the sky with respect to the galaxy and so the interstellar contribution was removed by averaging the results of all of the observed stars. The averaged Stokes parameters (λ 4400: $Q = 0.22 \pm 0.31$ per cent (internal standard deviation within sample), $U = -0.02 \pm 0.12$ per cent; λ 5900: $Q = 0.22 \pm 0.32$ per cent, $U = 0.03 \pm 0.12$ per cent) indicate a polarization $P = 0.22$ per cent, $\theta = 177°.4$ for the λ 4400 filter and $P = 0.22$ per cent, $\theta = 174°.0$ for the λ 5900 filter. The interstellar contribution was assumed to follow a Serkowski law with

$P_{max} = 0.23$ per cent, $\lambda_{max} = 5200$ Å with $\theta = 176°.0$. This contribution has been removed from the observations of Mrk 3 in all subsequent discussion and is small enough to cause no qualitative changes in the results for this galaxy.

For NGC 3516 one star (SAO 7270) does have detectable polarization in both filters. However, when the results for all stars are averaged, the resultant polarization is less than the typical error in the measurements of the galaxy polarization and so contributions from interstellar polarization have been neglected.

A search of the catalogues of linear polarization measurements of stars (Axon & Ellis 1976) reveals only one star with a galaxy–star separation of less than 7° with a distance greater than 150 pc. This star is HD 87737 which has a separation from NGC 3227 of 2°.7. It has a polarization of only 0.2 per cent, which, together with the observations of stars near NGC 3227 from Table 3, indicates that the interstellar polarization towards NGC 3227 is negligible.

## 4 Line polarization

The observed polarization of an emission line is contaminated by the polarization of the underlying continuum. We wish to determine the intrinsic polarization of the emission line flux in order to determine its source and to compare it to the continuum polarization.

The normalized Stokes parameter $Q_L$ and similarly $U_L$ for the emission line flux alone can be calculated from

$$Q_L = \frac{Q_{L+C} - Q_C(I_C/I_{L+C})}{1 - I_C/I_{L+C}}, \tag{1}$$

where $Q_{L+C}$ and $I_{L+C}$ are the measured line centre polarization and intensity respectively, and $Q_C$ and $I_C$ are the interpolated values of the same quantities at line centre.

The line intensity for the UWO data was measured from line scans made by tilting the interference filter used to isolate the line. This usually meant tilting the filters over a range of 15° because of the extreme widths of the emission lines. The transmission and bandwidth of an interference filter changes with incidence angle (Blifford 1966). This effect was measured for each line filter used by determining the bandwidth and transmission as a function of incidence angle with a monochromater. All estimates of the line intensities have been corrected for this effect. The corrections in every case were less than 10 per cent. The continuum polarizations at line centre were interpolated from the measurements with the adjacent continuum filters.

The line intensities for the MCSP observations were measured from the spectrophotometry, and the interpolated continuum polarizations are from the adjacent continuum channels.

The line intensities for the Digicon data were measured from the spectra in Figs 2(b) and 3(c). The continuum polarizations were determined by drawing a smooth curve through averaged data in regions of the spectra free of emission lines. This was straightforward for the NGC 3227 data but much of the continuum of Mrk 231 is badly contaminated by Fe II emission (Boksenberg *et al.* 1977).

For NGC 3227 the continuum regions were selected to be λλ 3920–4160, λλ 4160–4500, λλ 5400–4830, λλ 5100–5670, λλ 5670–6395 and λλ 6710–7100 (observed wavelengths). For Mrk 231 the regions were λλ 3900–3975, λλ 4100–4190, λλ 4200–4300, λλ 4875–4980, λλ 5270–5310, λλ 5810–5970, λλ 6240–6450 and λλ 7050–7570. Typical errors for these averaged data were about ± 0.15 per cent for regions to the red of ~ 4500 Å

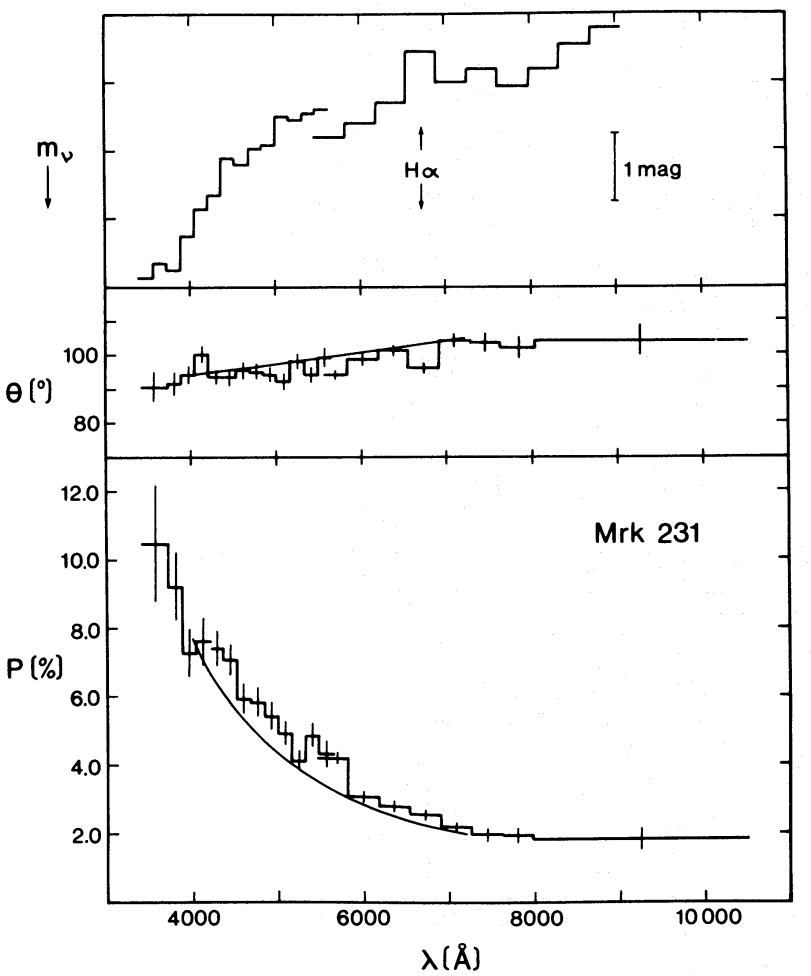


**Figure 2.** (a)

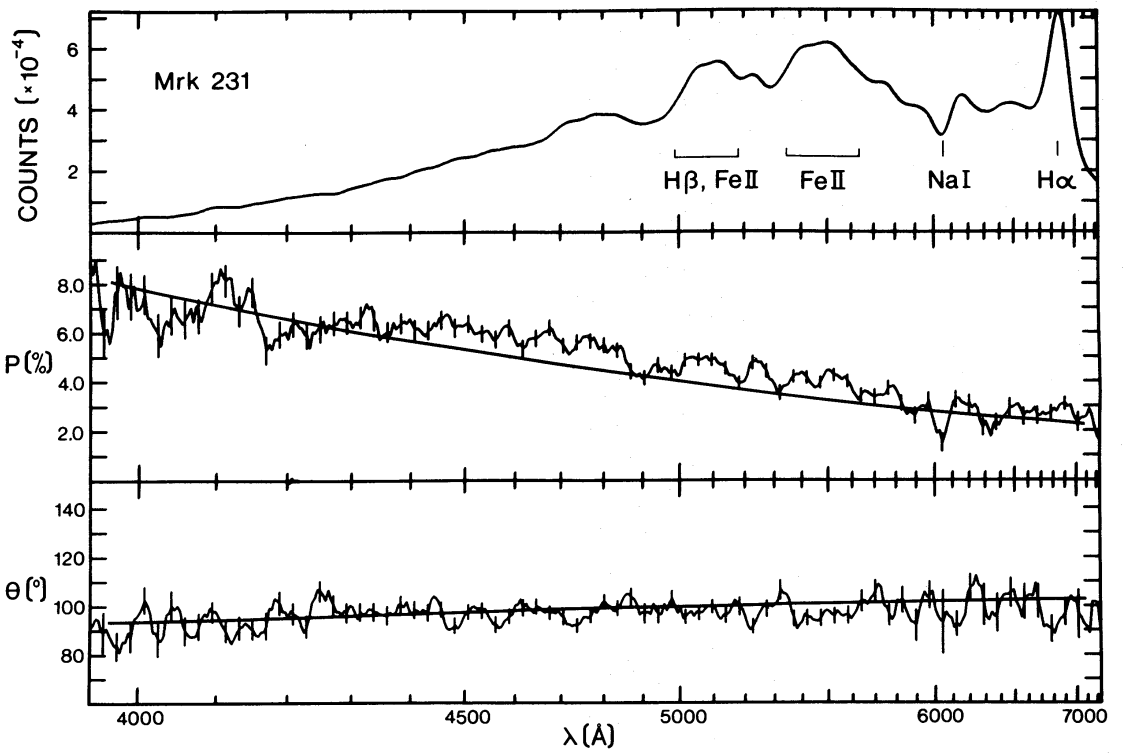


**Figure 2.** (b)

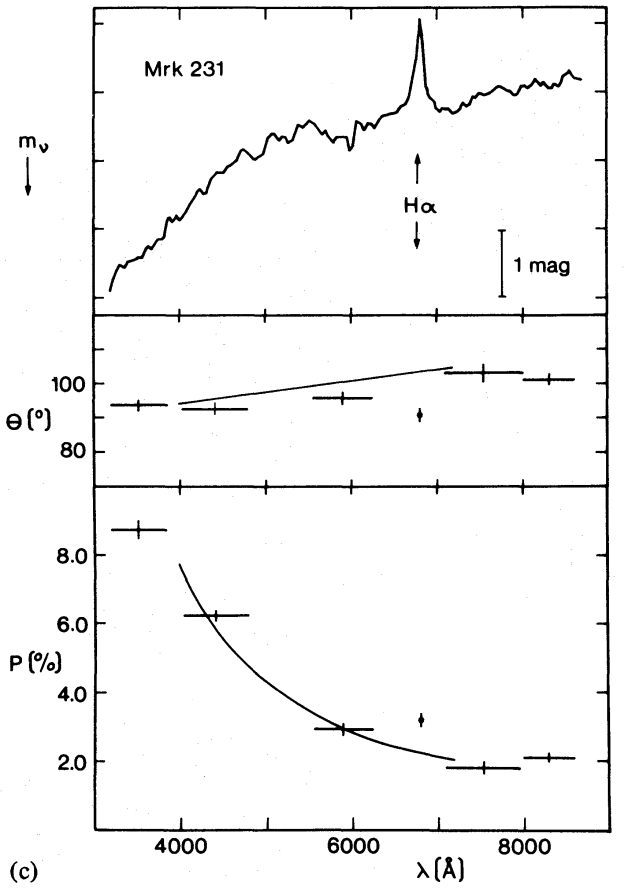


**Figure 2.** (a) MCSP observations of Mrk 231. The smooth curves for $P$ and $\theta$ are from the Digicon data for this galaxy (Fig. 2b). (b) Digicon observations of Mrk 231. The smooth curves for $P$ and $\theta$ are derived as described in Section 4. (c) UWO polarimeter observations of Mrk 231. The smooth curves for $P$ and $\theta$ are from the Digicon data for this galaxy (Fig. 2b).

and somewhat larger than this for regions to the blue of 4500 Å, leading to estimated errors in the adopted continuum polarizations of ±0.2 per cent. The adopted continuum polarizations and position angles are shown on the Digicon data in Fig. 2(b) (Mrk 231) and 3(a)

**Table 4.** Polarization of emission lines after subtraction of underlying continuum.

| Galaxy | Line | Instrument | $Q_C$ | $Q_L$ | $Q_C$-$Q_L$ | $U_C$ | $U_L$ | $U_C$-$U_L$ |
|---|---|---|---|---|---|---|---|---|
| Mrk 3 | [O III] | UWO | 0.57±0.12 | -0.46±0.22 | 1.03±0.25 | -1.71±0.12 | -0.74±0.22 | -0.97±0.25 |
| | Hα/[NII] | UWO | 0.01±0.09 | 0.39±0.23 | -0.38±0.25 | -1.28±0.09 | -1.03±0.23 | -0.25±0.25 |
| | Hα | UWO | 0.01±0.09 | 1.18±0.44 | -1.17±0.45 | -1.28±0.09 | -1.30±0.45 | 0.02±0.46 |
| Mrk 231 | Hα | Digicon | -2.02±0.20 | -3.49±0.33 | 1.47±0.39 | -0.88±0.40 | -0.33±0.61 | -0.55±0.73 |
| | Hα | MCSP | -2.19±0.13 | -2.79±0.21 | 0.60±0.25 | -0.98±0.12 | -0.09±0.21 | -0.89±0.24 |
| | Hα | UWO | -2.12±0.16 | -3.49±0.26 | 1.37±0.30 | -0.76±0.15 | 0.21±0.26 | -0.97±0.31 |
| | Average | | -2.13±0.09 | -3.15±0.15 | 1.02±0.17 | -0.89±0.09 | 0.01±0.16 | -0.90±0.18 |
| | Fe II*Hβ | Digicon | -4.01±0.20 | -5.66±0.37 | 1.65±0.42 | -1.27±0.40 | -0.49±0.72 | -0.78±0.75 |
| | Fe II† | Digicon | -3.48±0.20 | -4.85±0.30 | 1.41±0.36 | -1.18±0.40 | -0.21±0.59 | -0.97±0.62 |
| NGC 3227 | [O III] | Digicon | -0.16±0.20 | -0.31±0.45 | 0.15±0.49 | -1.55±0.20 | -1.43±0.52 | -0.12±0.56 |
| | [O III] | UWO | -0.18±0.09 | -0.66±0.30 | 0.46±0.32 | -1.57±0.09 | -1.15±0.32 | -0.45±0.34 |
| | Average | | -0.18±0.08 | -0.55±0.25 | 0.37±0.27 | -1.57±0.08 | -1.23±0.27 | -0.36±0.29 |
| | Hα | Digicon | -0.08±0.20 | -0.20±0.45 | 0.12±0.49 | -0.80±0.20 | -0.51±0.54 | -0.29±0.56 |
| | Hα | UWO | -0.16±0.10 | -0.40±0.23 | 0.24±0.25 | -0.74±0.10 | -0.74±0.22 | 0.01±0.24 |
| | Average | | -0.14±0.09 | -0.36±0.20 | 0.22±0.22 | -0.75±0.09 | -0.71±0.20 | -0.04±0.22 |
| NGC 3516 | Hα | MCSP | 0.55±0.10 | 0.68±0.10 | -0.13±0.14 | 0.05±0.10 | -0.04±0.10 | 0.09±0.14 |

* Fe II multiplet #42, † Fe II multiplets #42, 48, 49

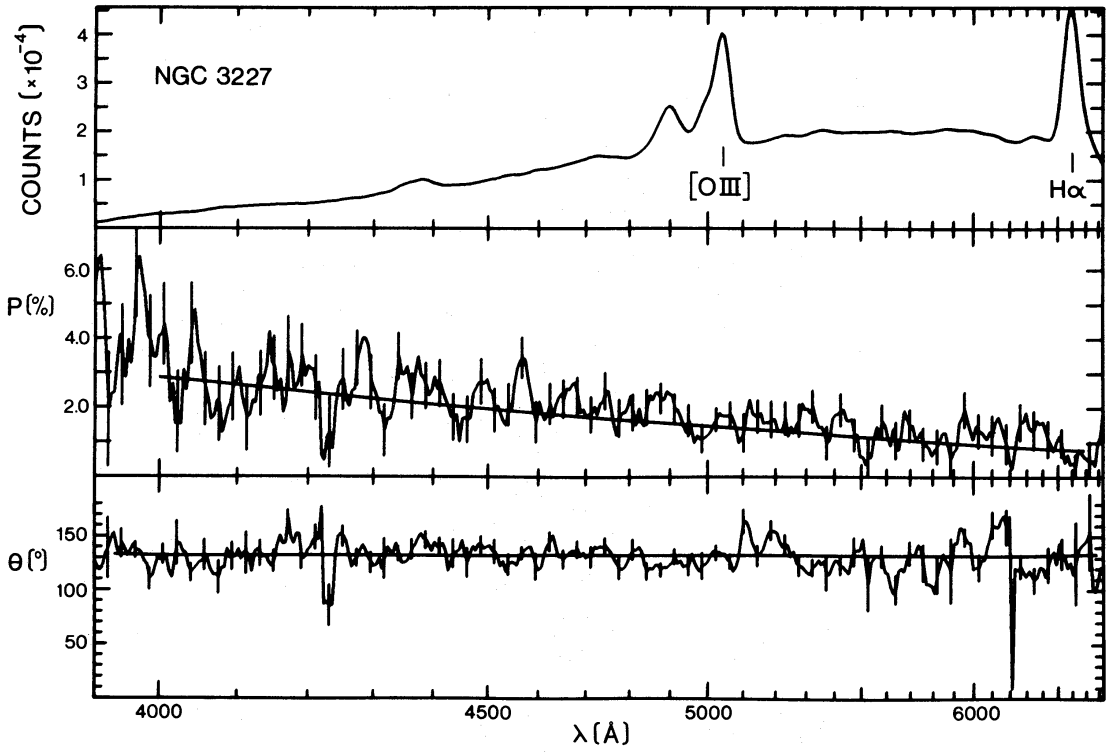


(a)

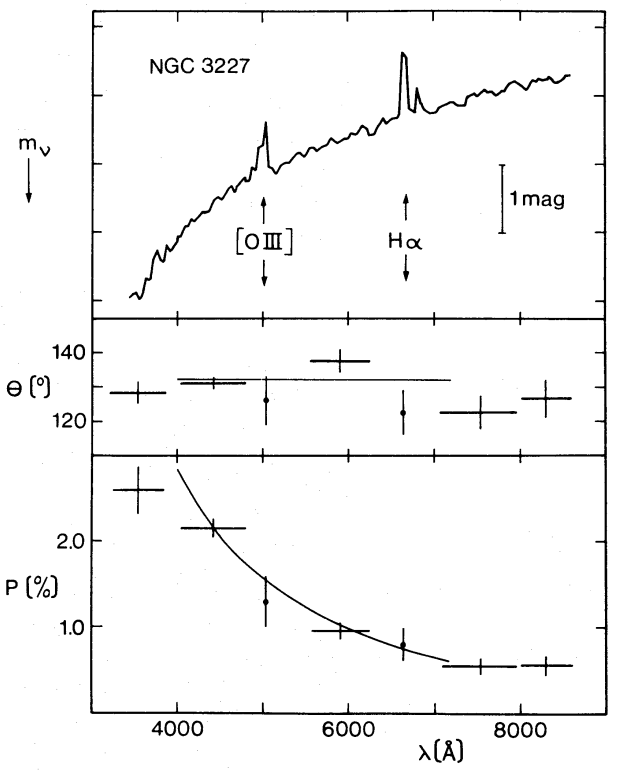


(b)

**Figure 3.** (a) Digicon observations of NGC 3227. The smooth curves for $P$ and $\theta$ are derived as described in Section 4. The features in the position angle plot at ~4230 and ~6200 Å are statistical fluctuations in the data, and are caused by low values of the polarization at these points. (b) UWO polarimeter observations of NGC 3227. The smooth curves for $P$ and $\theta$ are from the Digicon data for this galaxy (a). The spectrophotometry is from de Bruyn & Sargent (1978).

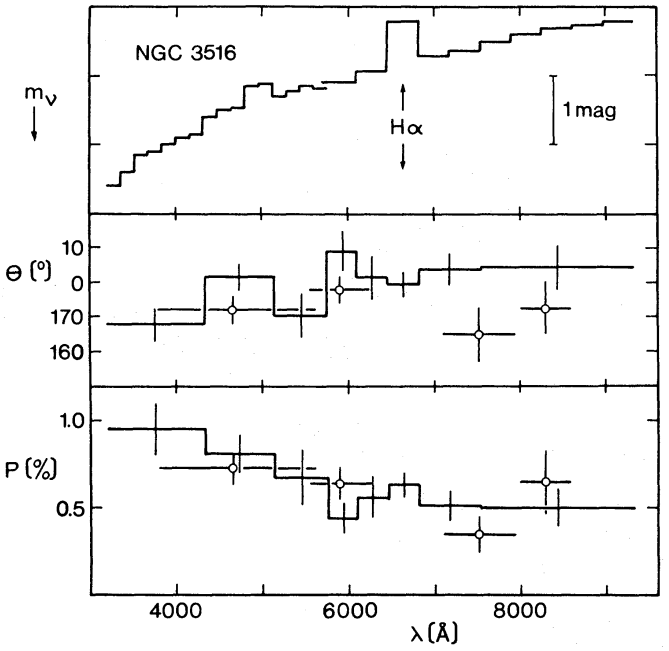


**Figure 4.** Observations of NGC 3516. The MCSP data is represented by the histogram and the UWO data by the circles.

(NGC 3227). The curves in Figs 2(b) and 3(a) fit the averaged data points to better than 0.1 per cent. The curves are included in the figures of the UWO and MSCP data of these two galaxies for comparison.

The Stokes parameters for the line emission alone are given in Table 4 where they are compared to the local continuum values. (Note that the corrections to the observed values caused by the galactic interstellar polarization do not affect these comparisons as the corrections apply to both the line and continuum polarization.) For each galaxy there are no significant variations in the line polarization measured with different instruments and so the data have been averaged. The reduced continuum and line polarizations from these averaged values are presented in Table 4. The quoted errors for all of the line polarizations include a contribution for the uncertainty in the relevant continuum polarizations. Individual galaxies are discussed below.

### 4.1 MRK 3

The [O III] λ 5007 polarization is lower than the continuum polarization and there is a rotation in the position angle ($P_L = 0.84 \pm 0.22$ per cent, $\theta_L = 119°.1 \pm 7°.5$; $P_C = 1.80 \pm 0.12$ per cent, $\theta_C = 144°.2 \pm 1°.9$). This is similar to the situation observed in the Seyfert galaxy NGC 1068 (Angel *et al.* 1976). Contributions to the observed Hα profile from the [N II] λλ 6548, 6584 emission lines in the four observed galaxies are small in all cases except Mrk 3 (Boksenberg *et al.* 1977; Osterbrock 1977; Koski 1978) and so the derived Hα polarizations for Mrk 231, NGC 3227 and 3516 are not contaminated by any [N II] polarization. The [N II] contribution in Mrk 3 for these observations was estimated from the Hα and [N II] relative line strengths observed by Koski (1978) assuming that the lines have Gaussian profiles with FWHP values of 900 km $s^{-1}$. The Hα/[N II] ratio within the bandpass of the interference filter used for the Hα line polarization observations is 1.1. The polarization for the Hα flux alone can be found using a relation similar to equation (1) if it is assumed that the [N II] polarization is the same as the value for the [O III] emission.

The derived Hα polarization is $P = 1.70 \pm 0.45$ per cent, $\theta = 156°.1 \pm 7°.5$ compared to a continuum value of $P = 1.28 \pm 0.09$ per cent, $\theta = 135°.2 \pm 2°.1$. (If the forbidden line polarization in this galaxy is caused by dust scattering or dust transmission – see Section 6 – then the [N II] λλ 6548, 6584 polarization is expected to be less than the [O III] λ 5007 polarization because of the difference in wavelength of the two lines. This has the effect of slightly increasing the derived Hα polarization and rotating the position angle closer to the continuum value.) Thus the Hα polarization is the same as the continuum value to within the errors.

### 4.2 MRK 231

All three sets of data show that the Hα flux is polarized to a higher degree and at a different position angle than the continuum. The average of the Hα data gives $P_L = 3.15 \pm 0.16$ per cent, $\theta_L = 89°.9 \pm 1°.5$; $P_C = 2.31 \pm 0.09$ per cent, $\theta_C = 101°.3 \pm 1°.1$. This increase in the line polarization with respect to the continuum is also evident in the Digicon data for the blend of H and Fe II (multiplet 42) and the blend of Fe II multiplets 42, 48 and 49 (see Table 4). In each case the value of $Q_L$ differs from $Q_C$ by $3.9\sigma$, and, while the errors for $U_L$ are large, the sense of the rotation with respect to the continuum is the same as for the Hα data.

The Digicon data shows that the observed polarization drops sharply through the Na I *D* absorption present at wavelengths of 6047 and 6053 Å (Boksenberg *et al.* 1977). Fig. 5 shows the region of the absorption on an increased scale with the data smoothed with a three-point running mean. The continuum polarization and position angle curves are drawn as in Fig. 2. The drop in polarization is present with no change in position angle: at the deepest point in the absorption line $P = 0.95 \pm 0.57$ per cent, $\theta = 103°.3 \pm 22°.2$ compared to a continuum value of $P = 2.80 \pm 0.20$ per cent, $\theta = 100°.7 \pm 2°.1$. The data shown in Fig. 2(b) also suggest that the polarization drops near the Ca II *H* and *K* absorption lines at observed wavelengths of 4070 and 4040 Å, respectively. These absorption lines are in the same redshift system as the Na I lines (Boksenberg *et al.* 1977). Also suggested in Fig. 5 is an increase in the polarization of the λ 5876 He I flux coupled with a drop in the position angle, consistent with the results for the Fe II and Hα emission lines.

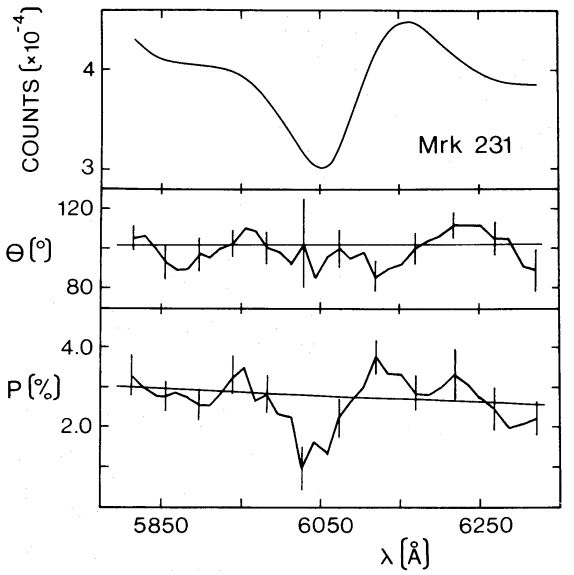


**Figure 5.** Digicon observations of Mrk 231 in the region of the Na I absorption. The data have been smoothed by a three-point running mean. The smooth curves for $P$ and $\theta$ are drawn as in Fig. 2(b).

**Table 5.** Average line and continuum polarization.

| Galaxy | Line | $P_L$ | $\theta_L$ | $P_C$ | $\theta_C$ |
|---|---|---|---|---|---|
| Mrk 3 | [O III] | 0.84±0.22 | 119.1±7.5 | 1.80±0.12 | 144.2±1.9 |
| | Hα | 1.70±0.44 | 156.1±7.5 | 1.28±0.09 | 135.2±2.0 |
| Mrk 231 | Hα | 3.15±0.16 | 89.9±1.5 | 2.31±0.09 | 101.3±1.1 |
| | Fe II, Hβ | 5.67±0.40 | 92.5±3.6 | 4.20±0.30 | 98.8±2.7 |
| | Fe II | 4.85±0.30 | 91.2±3.5 | 3.62±0.30 | 99.5±3.2 |
| NGC 3227 | [O III] | 1.32±0.26 | 123.0±5.6 | 1.58±0.08 | 131.7±1.5 |
| | Hα | 0.77±0.20 | 121.6±7.4 | 0.76±0.09 | 129.7±3.2 |
| NGC 3516 | Hα | 0.67±0.10 | 178.3±4.3 | 0.54±0.10 | 2.6±5.3 |

### 4.3 NGC 3227 AND 3516

The data in Table 5 show that both the λ 5007 [O III] and Hα emission lines in NGC 3227 are polarized the same as the continuum. This is the first Seyfert for which the forbidden lines have been found to be polarized as the continuum is. Digicon data for Hβ, for which the observational errors are large, are consistent with this line being polarized the same as the continuum.

The MCSP results for NGC 3516 show that the Hα flux is polarized and to within the errors the polarization is the same as for the continuum.

## 5 Continuum polarization

In our observations, we have also obtained detailed information about the continuum polarization. The behaviour of the continuum polarization, its wavelength dependence in strength and position angle, and its temporal dependence, can yield further information about the origin of the polarization and the structure of the nuclear regions.

### 5.1 VARIATION OF POLARIZATION WITH WAVELENGTH

Each of the four galaxies show a smooth increase of the polarization towards shorter wavelengths. Only for NGC 3227 is there any indication that the polarization curve is beginning to flatten into the UV. No observations with the λ 3500 filter were obtained for Mrk 3 but Maza (1979) reports a polarization of 2.83 ± 0.38 per cent, $\theta = 152°.2 \pm 4°.0$ in the wavelength region of 3200–4200 Å, consistent with the polarization rising smoothly into the UV. To show the sharpness of this increase in polarization and the degree of polarization, it is convenient to fit the continuum observations to a relationship of the form $P(\lambda) = P(5000\text{ Å})\ (\lambda/5000\text{ Å})^{-\alpha}$. For each galaxy, the data can be fitted to within the errors with

**Table 6.** Continuum polarization.

| Galaxy | P(3300Å) | P(5000Å) | P(7000Å) | $\frac{P(3300Å)}{P(5000Å)}$ | α |
|---|---|---|---|---|---|
| Mrk 3 | 3.3 | 1.9 | 1.2 | 1.7 | 1.4 |
| Mrk 231 | 11.0 | 4.2 | 2.1 | 2.9 | 2.3 |
| NGC 3227 | 3.2 | 1.4 | 0.7 | 2.3 | 2.0 |
| NGC 3516 | 1.0 | 0.7 | 0.5 | 1.4 | 1.1 |

such a curve. Table 6 presents the values of $P$(3300 Å), $P$(5000 Å), $P$(7000 Å), $\alpha$ and $P$(3300 Å)/$P$(5000 Å). The data are taken from the UWO observations. The value of $\alpha$ is accurate to approximately ± 0.2 and so it is clear from Table 6 that there is a real variation from galaxy to galaxy in the slope of the continuum polarization as well as in the level of the polarization.

### 5.2 VARIATION OF POSITION ANGLE WITH WAVELENGTH

Both sets of data for NGC 3227 are consistent with the position angle of the polarization being constant at 132°. For NGC 3516 there is some suggestion of a rotation of the position angle in the MCSP data but this is not supported by the UWO data. However, both Mrk 3 and Mrk 231 do show significant rotation of the position angle from short to long wavelengths. In the case of Mrk 3, the λ 4400 measurement ($\theta = 150°.2 \pm 1°.9$) differs from the λ 5900 measurement ($\theta = 134°.6 \pm 1°.7$) by $15°.6 \pm 2°.5$. The reality of this rotation is supported by the data from Maza (1979) quoted in Section 5.1 where $\theta = 152°.2 \pm 4°.0$ in the blue. The position angle appears to remain constant longward of 6000 Å. There is also a rotation of the position angle in Mrk 231 which is present in all three sets of data. The total amount of rotation is $\simeq 10°$ from 4000 Å ($\theta \sim 93°$) to 8000 Å ($\theta \sim 103°$). This gradual increase in the position angle is reversed at longer wavelengths. Observations by Kemp *et al.* (1977) show that $\theta = 94° \pm 6°$ at 1.6 μm and $\theta = 77° \pm 6°$ at 2.2 μm.

There is no relation between the observed polarization position angles and the position angles of the optical images of the galaxies as given by Nilson (1973) for Mrk 231, NGC 3227 and 3516 or as measured from the photograph of Mrk 3 given by Weedman (1973).

### 5.3 TEMPORAL VARIATIONS

As is outlined in Table 2, the data on the four galaxies have been obtained over the time interval 1975–79, and so time bases from a few days to 3 yr are available to search for possible polarization variations with time.

For Mrk 231, NGC 3227 and 3516, all of the data that have been obtained are plotted in Figs 2–4 and the lack of variations is obvious from those figures. The apparent discrepancy for Mrk 231 between the MCSP observations and the adopted Digicon continuum can be explained by the effect of the Fe II emission on the polarization. The two agree in the regions free of emission lines.

For Mrk 3, five different observations were obtained with the λ 5900 filter and the maximum variation from the mean used in Fig. 1 is less than 2 $\sigma$, consistent with constant polarization.

These data are also consistent with the observations of these four galaxies by Maza (1979) when differences in spectral resolution are taken into account. Thus no significant time variations in the polarization of any of these galaxies have been observed.

## 6 Discussion

### 6.1 MODELS FOR THE POLARIZATION

Several possible sources for the observed polarization may be considered. (1) The polarization may be evidence for non-thermal radiation from the central source. In this case, the polarization would probably be independent of wavelength as is observed for some BL Lac objects (e.g. BL Lac: Knacke, Capps & Johns 1976; OJ 287: Maza, Martin & Angel 1978)

and OVV QSOs (Visvanathan 1973). However, a decrease in the polarization towards the red can also be produced from a flat wavelength dependence by dilution by starlight if the active object is embedded in a 'host' galaxy (Maza, Martin & Angel 1978). In either case, any emission lines produced in the central object are expected to be unpolarized. (2) Polarization could be caused by aligned grains between the Seyfert nucleus and ourselves, either in our own Galaxy (already discounted or corrected for in Section 3) or in the nuclear bulge of the Seyfert galaxy. In this case, the polarization wavelength dependence would probably follow the form found in our own galaxy, which is described by the Serkowski formula (Serkowski, Mathewson & Ford 1975). The emission line flux for both permitted and forbidden lines would have the same polarization as the continuum. (3) Polarization could arise from scattering by free electrons in the gas clouds around the central source, as occurs in Be stars. We would expect to find a wavelength dependence which is either flat or which is lower on the short wavelength side of the Balmer jump than on the long wavelength side, due to a competition between electron scattering and hydrogen absorption. As in (1), the wavelength dependence can be altered by a stellar contribution which varies with wavelength. The emission lines, which arise in the same gas which scatters the continuum radiation, would be nearly unpolarized. (4) Finally, the polarization could be due to scattering of the continuum radiation by an asymmetric distribution of dust grains in the neighbourhood of the nucleus. If the dust grains are small ($\lesssim 0.1\ \mu$m) the continuum polarization would rise sharply to shorter wavelengths, while a flatter dependence would be produced by larger grains. In this case as well, the continuum polarization could be affected by starlight from regions outside of the dust cloud. The line polarization would depend on the location of the dust cloud with respect to the line emitting regions. Line flux emitted close to the nucleus would have the same polarization as the continuum while line flux arising outside of the dust cloud would be largely unpolarized.

The emission line and continuum data presented here strongly support the conclusion that for each galaxy in our sample the polarization is caused by dust scattering in asymmetrically distributed clouds surrounding the nucleus. The following points support this view:

(a) In all cases the emission lines were found to be polarized similar to the continuum. This eliminates electron scattering and non-thermal mechanisms. In addition, the drop in polarization through the Na I *D* absorption in Mrk 231 and the low [O III] $\lambda$ 5007 polarization in Mrk 3 indicates that transmission by aligned dust grains cannot be responsible for the polarization in these two galaxies.

(b) The wavelength dependence of the continuum polarization in NGC 3227 and 3516 can be approximately fitted with a Serkowski interstellar curve with the parameters $\lambda_{max} =$ 2250 Å, $P_{max} = 3.3$ per cent and $\lambda_{max} = 3400$ Å, $P_{max} = 0.9$ per cent, respectively. These extremely low values of $\lambda_{max}$ imply that the characteristics of the polarizing grains in these galaxies must be much different than the characteristics of the grains in our Galaxy. Data in Serkowski, Mathewson & Ford (1975) indicate that for ~ 350 stars in our own Galaxy with well determined interstellar polarization, all have $\lambda_{max} > 4500$ Å. Thus, unless the grain properties are very different from those in our own Galaxy, we can also eliminate transmission through aligned grains as a polarizing mechanism.

We now consider the nature of the scattering clouds and the implications of these dust clouds for each object.

Shawl (1975) has described models of polarization produced by scattering in optically thin, asymmetric dust clouds surrounding a central point source of radiation. The wavelength dependence of the polarization in the four galaxies observed can be reproduced by such models when the dust particles are silicates with radii less than ~ 0.07 $\mu$m, with the

flatter polarization spectrum of NGC 3516 perhaps indicating a wide mixture of particle sizes. However, these models typically can produce a maximum value of only ~ 1.1 per cent for the polarization at 5000 Å. With the exception of NGC 3516, all of the observed galaxies significantly exceed this value. It is possible to increase the value of the polarization in these models by selectively blocking our direct view of the continuum light (perhaps with optically thick dust clouds) to allow scattered light to dominate. In this case, one would expect both continuum flux and polarization variations as mass motions in the nucleus carried the blocking clouds out of the line-of-sight to the nucleus. Light variations have been observed only in NGC 3516 and there are no reported polarization variations (see Section 5.3), but the time-scale of the observations may as yet be too short.

Optically thick scattering in asymmetric dust clouds can reproduce both the degree of polarization at 5000 Å and the wavelength dependence (Daniel 1978). Typical optical depths for appropriate models range from 2 to 4 at 3300 Å with silicate particle radii of 0.05 $\mu$m in a disc-like geometry. There is indeed evidence for high extinction in those galaxies with high polarization. In Mrk 231, the 10 $\mu$m silicate feature has been detected in absorption with $\tau \sim 0.8$, implying an extinction of $A_V \sim 18$ in the dust clouds (Rieke 1976). The continuum and emission lines appear to be reddened by $A_V \sim 2.1$ and, assuming normal abundances and an interstellar gas-to-dust ratio, the non-stellar Ca II and Na I absorption lines both imply an extinction of $A_V \sim 2$ (Boksenberg *et al.* 1977). In NGC 3227 the silicate feature has been detected in absorption with an optical depth of 0.5, implying an extinction of $A_V \sim 11$ (Lebofsky & Rieke 1979). The H$\alpha$/H$\beta$ ratio in this galaxy (Osterbrock 1977) implies an extinction of $A_V \sim 1.3$, although there is considerable disagreement in the literature as to the value of this ratio (Anderson 1970; Wampler 1971; Adams & Weedman 1975). These earlier measurements suggest a higher degree of reddening. Variability in the strengths of the hydrogen lines in this galaxy is a possibility. In Mrk 3 the Balmer decrement agrees with that predicted by case B recombination reddened by $A_V = 1.5$ (Koski 1978).

The three Seyferts known to have pronounced 10 $\mu$m absorption (NGC 1068), Kleinmann, Gillette & Wright (1976); Mrk 231 and NGC 3227) all have lower values of $A_V$ from optical estimates than from the strength of the 10 $\mu$m feature. It must be emphasized that the optical estimates of the extinction are only lower limits for those dust particles with non-zero albedo (Jones 1973; Jones & Stein 1975). Since we are not resolving the nuclei of these galaxies, light is scattered back into our line-of-sight producing an effective extinction which is lower than the true geometrical extinction. The fact that a considerable fraction of the light is scattered in the optical in these three galaxies is demonstrated by the existence of high polarization in each of these galaxies. Note also that if the emitting gas is mixed with the dust then estimating the amount of reddening from the Balmer decrement will only give a lower limit to the reddening on the line-of-sight to the central source (Jones & Stein 1975).

### 6.2. MRK 231

Boksenberg *et al.* (1977) show that the optical continuum of Mrk 231 can be well fitted with a $10^4$K blackbody (representative of early type stars) reddened by $A_V = 2.1$ mag. Attempts to fit the continuum with a reddened power law spectra produced a 20–30 per cent deficiency in the flux in the region 4000–6000 Å. The presence of absorption lines of the Balmer series together with the Ca II *K* line at the redshift of the galaxy with equivalent widths consistent with A0 stars supports the interpretation that the optical continuum is strongly dominated by starlight. For the continuum to have the observed polarization, a large fraction of the stars in the nucleus must be within the polarizing dust cloud.

The continuum polarization drops smoothly into the infrared with $P = 0.98 \pm 1.18$ per cent at 1.6 $\mu$m and $P = 0.55 \pm 0.11$ per cent at 2.2 $\mu$m, while, as mentioned in Section 5.2, the sense of rotation of the position angle through the optical reverses with $\theta = 94^\circ \pm 6^\circ$ at 1.6 $\mu$m and $\theta = 77^\circ \pm 6^\circ$ at 2.2 $\mu$m (Kemp *et al.* 1977). This behaviour of the position angle is remarkably similar to that observed in NGC 1068: in both cases there is a rotation of $\sim 10^\circ$ from 3500 to 8500 Å, where the sense of rotation reverses, followed by a rotation of $\sim 20^\circ$–$25^\circ$ from 9000 Å to 2.2 $\mu$m (Angel *et al.* 1976; Lebofsky, Rieke & Kemp 1978). However, for NGC 1068, the polarization increases from $\sim 1$ per cent at 9000 Å to $\sim 4$ per cent at 2.2 $\mu$m. The optical polarization in each case is produced by scattering in dust clouds around the nucleus with the rotation of the position angle likely produced by optical depth effects similar to those observed in the heavily reddened stars VY CMa and NML Cyg (Serkowski 1973; Angel & Martin 1973). Evidence in support of this interpretation is the detection of optical circular polarization in NGC 1068, where the eccentricity increases strongly into the red, as is observed in VY MCa and NML Cyg. Optical circular polarization is not observed in Mrk 231: Maza (1979) has placed upper limits of 0.16 per cent in the wavelength range 3330–4170 Å and 0.07 per cent in the wavelength range 5560–8330 Å.

Lebofsky, Rieke & Kemp (1978) suggested that the increase in polarization towards 2 $\mu$m in NGC 1068 coupled with the change in position angle is evidence for a central non-thermal source which can only be seen between 1 and 5 $\mu$m. In this model the central source is polarized at a constant level at a different position angle from that resulting from the scatterers, producing the observed polarization wavelength dependence together with the position angle rotation as the central source begins to dominate redward of 1 $\mu$m. As mentioned above, there is not a similar increase in the infrared polarization of Mrk 231. This may, however, be caused by the large observing apertures used in the infrared polarization measurements. The 2.2 $\mu$m observations were made with a 7.8 arcsec aperture which projects to a 8.4 kpc radius at Mrk 231, large enough to cause considerable dilution by cool stars external to the nucleus. It would be valuable to do multiaperture photometry and polarimetry in the infrared to check this possibility. Dilutions by a factor of $\sim 7$ would produce a polarization at 2.2 $\mu$m similar to that observed in NGC 1068.

If dilution is not important, an alternate explanation of the polarization and position angle wavelength dependence in Mrk 231 and NGC 1068 is that there is an unpolarized central source, presumably non-thermal, that is so obscured that it can only be detected in the wavelength region 1–5 $\mu$m. The existence of such a source is suggested if the Ca II triplet and Fe II emission is produced by fluorescence (Boksenberg *et al.* 1977). This source would view the polarizing dust from a different aspect than the stars which produce the observed optical continuum and this might cause a rotation of the position angle as the central source becomes increasingly dominant to the red of 1 $\mu$m. The drop in polarization towards the infrared is produced by the characteristics of the polarizing dust. This explanation is supported by the position angle of the emission line polarization. The emission lines can be expected to arise from ionized clouds close to the central source. As a result they would illuminate the dust from an aspect similar to that of the nuclear source. The same situation is suggested in NGC 1068 where the position angle of the H$\alpha$ emission is rotated from the local continuum in the same sense as the polarization at 2.2 $\mu$m (Angel *et al.* 1976).

If there is no central non-thermal source then the rotation of the position angle must be caused by optical depth effects. Light at longer wavelengths penetrates farther into the dust cloud with the scattering plane varying with position in the cloud.

Boksenberg *et al.* (1977) have discussed the Na I *D* absorption lines in Mrk 231. The lines are blue-shifted by 4600 km $s^{-1}$ with respect to the emission lines and are apparently formed

by discrete gas clouds in front of the nucleus. Although the lines have an apparent optical depth of 30 as determined from line ratios, there is residual flux in the cores of the lines amounting to ~ 30 per cent of the continuum. This extra flux was suggested by Boksenberg *et al.* to be either light from the nucleus leaking through holes in the absorbing cloud, light from stars external to the absorbing cloud, or flux from the wings of the He I λ 5876 emission line. These observations of the Na I absorption, together with the polarization data, may be used to constrain the location and distribution of the absorbing cloud.

Our Digicon observations are consistent with zero polarization in the cores of the lines. The measured polarization in the three-point mean at the line core is 0.95 ± 0.57 per cent (see Fig. 5), whereas the polarization of the nearby continuum is ~ 3 per cent. Models in which the absorption is produced in a single cloud which obscures only the nucleus but not the scattering clouds are ruled out. In this case much of the residual flux in the line core would be scattered light from the other clouds and the polarization would be expected to increase through the absorption line. To produce a drop in the polarization, the absorbing cloud must cover the entire nucleus/line emitting region/dust cloud complex, or it must prevent nuclear light (with wavelength ~ redshifted Na I *D*) from reaching the dust scatterers. The first possibility is ruled out by the He I λ 3889 absorption at the same redshift as the Na I *D* lines. As Boksenberg *et al.* (1977) mention, the presence of Na I and He I line absorption at the same redshift strongly suggests that the absorbing cloud is being illuminated by a dilute, unreddened radiation field with a high colour temperature. Since the scattering clouds responsible for the polarization should also redden the nuclear light, they cannot be inside the Na I absorbing cloud. Thus the most favourable model has the line absorbing cloud interior to or coincident with the scattering cloud. In either case, it is unlikely that the residual flux at line core is He I λ 5876 emission or light escaping through holes in the absorbing cloud since both would be expected to be polarized. The most reasonable explanation for the excess flux is starlight which originates outside of the dust cloud. This starlight also provides a natural explanation for the higher degree of polarization observed for the emission line flux. Since this excess flux is unpolarized, it will dilute the intrinsic polarization of the radiation escaping the absorbing dust complex. As a result, the emission lines, whose relative dilution will be less than that of the continuum, should show higher polarization. Using the observed polarization and flux of Hα and the nearby continuum, and assuming the increased polarization in Hα to be solely due to this effect, we require the excess flux of starlight to be 32 per cent of the continuum at Hα. The data of Boksenberg *et al.* indicate a value of 30 per cent for the remaining flux in the Na I *D* lines if the extra flux in the cores of the lines is polarized, as our observations show. Considering the rotation of the position angles of the line polarization compared to the continuum polarization and the difference in wavelengths between Hα and Na I *D*, such an excellent agreement may well be fortuitous. However, it does suggest that dilution by starlight external to the nucleus is important to Mrk 231.

The general picture of the nucleus of Mrk 231 that is suggested by the polarimetric observations is as follows. The central portion of the nucleus consists of a non-thermal source surrounded by ionized gas which produces the emission lines. These are centred in a distribution of hot stars giving the optical continuum and all is encompassed in a series of absorbing clouds responsible for the absorption lines. This entire distribution of material is roughly centred in an asymmetric dust cloud which produces the polarization. At Hα, some 30 per cent of the optical continuum is in the form of starlight from outside the dust cloud. The [O II] λ 3727 emission is extended (Adams 1972) and presumably lies outside the dust. As a result, this emission should be unpolarized. Polarimetric observations of the absorption lines of Na I and He I in the $v = 6250$ km s$^{-1}$ redshift system would be useful in further determining the distribution of material in the nucleus of Mrk 231.

### 6.3 MRK 3

Observations of the optical spectrum of this object are given by Koski (1978), Neugebauer *et al.* (1976) and de Bruyn & Sargent (1978) and infrared photometry is given by Rieke (1978), Neugebauer *et al.* (1976) and McAlary, McLaren & Crabtree (1979). Koski shows that the optical continuum is consistent with a stellar continuum together with a power law with index $-0.7$. The stellar continuum contributes ~ 80 per cent of the total flux at H$\alpha$, while the contribution is closer to ~ 50 per cent at 3500 Å where there may be additional flux from the Balmer continuum. The infrared flux drops from 1.6 to 3.5 $\mu$m, consistent with the spectrum of cool stars, and then rises to at least 20 $\mu$m, consistent with a cool blackbody, presumably thermal emission from dust. An extension of the optical power law with index $-0.7$ to infrared wavelengths falls well below the observed flux levels. There have been no observations of the 10 $\mu$m dust feature.

The continuum flux at H$\alpha$ is strongly dominated by starlight and the similarity of the H$\alpha$ polarization and the continuum polarization suggests that a large fraction of the stars must be within the polarizing dust. The [O III] $\lambda$ 5007 emission is polarized less than the continuum and this suggests that the emission is produced in clouds that are external to or coincident with the polarizing dust, as is the case for NGC 1068 (Angel *et al.* 1976). This is consistent with the detection of forbidden line flux external to the nucleus (Balick & Heckman 1979; Weedman 1973), as discussed in Section 2. The rotation of the position angle of the polarization at short wavelengths may be caused by optical depth effects or by the increasing dominance of the underlying power law continuum which may be intrinsically polarized or may view the surrounding polarizing dust from a different perspective. Maza (1979) has placed a $3\sigma$ upper limit of 0.07 per cent on the circular polarization in the wavelength range 3330–8330 Å.

Thus in Mrk 3 we have a situation in which there is a central source, presumably non-thermal, surrounded by a distribution of stars and emitting gas. This in turn is surrounded by an asymmetric dust cloud and then by gas clouds responsible for the forbidden line radiation.

### 6.4 NGC 3227

Observations of the optical spectrum of NGC 3227 have been given by de Bruyn & Sargent (1978), Osterbrock (1977) and infrared photometry by Rieke (1978) and McAlary, McLaren & Crabtree (1979). Osterbrock (1978) estimates that stars contribute only ~ 10 per cent of the flux at H$\beta$ and that the continuum is strongly dominated by a non-stellar power law. This is supported by the near infrared photometry which shows only a shallow decrease in the flux from 1.6 to 3.5 $\mu$m, presumably indicating the strength of the non-stellar source even at these wavelengths (Neugebauer *et al.* 1976). The far infrared, however, is dominated by dust emission, as shown by the strength of the 10 $\mu$m feature (Lebofsky & Rieke 1979). The detection of the 10 $\mu$m feature is circumstantial evidence that the properties of the dust in this galaxy are similar to those of the dust grains in our own Galaxy, thus making the possibility that the polarization is caused by aligned interstellar grains unlikely (see Section 6.1).

The polarization data, which show similar polarization in the continuum, H$\alpha$ and [O III], indicate that the entire complex of continuum source and emitting gas clouds are surrounded by a common polarizing dust cloud. Since NGC 3227 is fairly close by, with a scale on the sky of only 1.01 kpc arcsec$^{-1}$ for $H_0 = 55$ km s$^{-1}$ Mpc$^{-1}$, the possibility exists of resolving the infrared emission on the sky if the emitting dust is also responsible for the

polarization and if the forbidden line emission is extended over distances from the nucleus that are comparable to those in NGC 1068 and Mrk 3.

### 6.5 NGC 3516

The optical spectrum of NGC 3516 has been described by Boksenberg & Netzer (1977) and Osterbrock (1977). Osterbrock (1978) states that within a 2.7 by 4.0 arcsec aperture, 14 per cent of the continuum at Hα is in the form of starlight. Furthermore, flux variations have been reported in the blue, but none are seen to the red of 5000 Å. These observations suggest that the continuum in the region of Hα is dominated by starlight. This is in agreement with the discussion of Boksenberg & Netzer (1977) and Collin-Souffrin, Alloin & Andrillat (1973). Since, within a similar diaphragm, the polarization Hα is the same as the continuum, the stars contributing to the continuum are also within the dust shell.

Although we detect the [O III] λ 5007 emission line in the MCSP spectrophotometry, the observational errors of the polarimetry of this line are too high to say whether or not the emission is polarized and hence whether the geometry is similar to NGC 3227 or to Mrk 3. The broad emission lines of Hα and Hβ also have narrow cores reminiscent of those in NGC 4151 (Boksenberg *et al.* 1975). These cores are presumably from the same low density gas that emits the forbidden lines. The Hα/Hβ ratio of 4.9 for these core components (Boksenberg & Netzer 1977) indicates that there is some reddening of this flux and if the reddening dust can be identified with the polarizing material then the scattering cloud must surround the entire emitting region. Note, however, that the broad line emission is not reddened by the same amount since the Hα flux and the Hα/Hβ ratio are both variable, the latter having values in the range from 2.94 (Osterbrock 1977) to 4.5–5.8 (Boksenberg & Netzer 1977). These variations are not caused by a change in the reddening as a dust cloud drifts in front of the nucleus (*cf.* the discussion of polarization variations in Section 6.1) since the [O III] λ 5007 flux has remained constant over the time period of the observations. Boksenberg & Netzer (1977) explain the variations as an effect of the variations of the central ionizing source coupled with self absorption of the Balmer lines in the dense emitting clouds.

Thus we can only say that the wavelength dependence and degree of polarization can be explained with either optically thin or optically thick dust scattering with the scatters surrounding at least the region responsible for the continuum at Hα and the dense clouds emitting the broad line emission.

## 7 Summary

We have found that the optical polarization of Mrk 3, Mrk 231, NGC 3227 and probably NGC 3516 is caused by scattering in asymmetric distributions of dust in the nuclei of these galaxies. The extent of this polarizing dust varies from galaxy to galaxy. Polarized permitted line radiation shows that in all four cases the dust is external to the permitted line emitting regions. The dust is contained within the forbidden line emitting regions in Mrk 3 and probably Mrk 231, and is outside of these regions in NGC 3227. The extent of the dust in NGC 3516 is uncertain. The observed polarization drops through the non-stellar Na I*D* line absorption in Mrk 231, suggesting that the absorption is formed in gas clouds within the polarizing dust. The existence of a central non-thermal source is indicated in Mrk 3 and Mrk 231 from the wavelength dependence of the position angle of polarization.

These observations, together with those of NGC 1068, IC 4329A and Mrk 376, show that in most Seyfert galaxies with polarization greater than ~ 1 per cent, dust scattering is the predominant polarizing mechanism. A major unanswered question is the relation between the dust that reddens the continuum and emission lines, that which produces the 10 $\mu$m absorption feature and that which produces the polarization. Observations of NGC 1068 (Angel *et al.* 1976; Woolf *et al.* 1976) give similar degrees of reddening for the permitted and forbidden line regions while the polarization properties of these two regions differ radically, indicating at least two different dust distributions. Our observations of Mrk 3 suggest that a similar situation exists in this galaxy. Measurements of the infrared (S II] lines, together with existing spectrophotometry of Seyferts, would allow the degree of reddening of the forbidden lines to be determined. Such observations, taken together with measurements of line and continuum polarization, would make a valuable contribution to our understanding of the distribution and role of dust in Seyfert nuclei.

## Acknowledgments

We would like to thank the Director of Hale Observatories for observing time, and Mira Rasche and Enid Goodall for help in preparing the manuscript. This work was supported by the National Research Council of Canada. The observations with the UCDS Digicon at Steward Observatory were supported by the NSF under grant AST 75-17845 and by NASA under grant NGR 05-009-188.

## References

Adams, T. F., 1972. *Astrophys. J.*, **176**, L1.
Adams, T. F. & Weedman, D. W., 1975. *Astrophys. J.*, **199**, 19.
Anderson, K. S., 1970. *Astrophys. J.*, **162**, 743.
Angel, J. R. P. & Landstreet, J. D., 1970a. *Astrophys. J.*, **160**, L147.
Angel, J. R. P. & Landstreet, J. D., 1970b. *Astrophys. J.*, **162**, L161.
Angel, J. R. P. & Landstreet, J. D., 1974. *Astrophys. J.*, **191**, 457.
Angel, J. R. P. & Martin, P. G., 1973. *Astrophys. J.*, 180, L39.
Angel, J. R. P., Stockman, H. S., Woolf, N. J., Beaver, E. A. & Martin, P. G., 1976. *Astrophys. J.*, **206**, L5.
Angel, J. R. P. *et al.*, 1978. *Proc. Pittsburgh Conference on BL Lac Objects*, p. 117, Pittsburgh, 1978 April 24–26.
Axon, D. J. & Ellis, R. S., 1976. *Mon. Not. R. astr. Soc.*, **177**, 499.
Balick, B. & Heckman, T., 1979. *Astr. J.*, **84**, 302.
Beaver, E. A., Harms, R., Hazard, C., Murdoch, H. S., Carswell, R. F. & Strittmatter, P. A., 1976. *Astrophys. J.*, **203**, L5.
Blifford, I. H., 1966. *Appl. Opt.*, **5**, 105.
Boksenberg, A. & Netzer, H., 1977. *Astrophys. J.*, **212**, 37.
Boksenberg, A., Carswell, R. F., Allen, P. A., Fosbury, R. A. E., Penston, M. V. & Sargent, W. L. W., 1977. *Mon. Not. R. astr. Soc.*, **178**, 451.
Boksenberg, A., Shortridge, K., Allen, D. A., Fosbury, R. A. E., Penston, M. V. & Savage, A., 1975. *Mon. Not. R. astr. Soc.*, **173**, 381.
Collin-Souffrin, S., Alloin, D. & Andrillat, Y., 1973. *Astr. Astrophys.*, **22**, 343.
Daniel, J.-Y., 1978. *Astr. Astrophys.*, **67**, 345.
de Bruyn, A. G. & Sargent, W. L. W., 1978. *Astr. J.*, **83**, 1257.
Jones, T. W., 1973. *Publs astr. Soc. Pacif.*, **85**, 811.
Jones, T. W. & Stein, W. A., 1975. *Astrophys. J.*, **197**, 297.
Kemp, J. C., Rieke, G. H., Lebofsky, M. T. & Coyne, G. V., 1977. *Astrophys. J.*, **215**, L107.
Kleinmann, D. E., Gillette, F. C. & Wright, E. L., 1976. *Astrophys. J.*, **208**, 42.
Knacke, R. F., Capps, R. W. & Johns, M., 1976. *Astrophys. J.*, **210**, L69.
Koski, A. T., 1978. *Astrophys. J.*, **223**, 56.

Landstreet, J. D. & Angel, J. R. P., 1977. *Astrophys. J.*, **211**, 825.
Lebofsky, M. J. & Rieke, G. H., 1979. *Astrophys. J.*, **229**, 111.
Lebofsky, M. J., Rieke, G. H. & Kemp, I. C., 1978. *Astrophys. J.*, **222**, 95.
Martin, P. G., Angel, J. R. P. & Maza, J., 1976. *Astrophys. J.*, **209**, L21.
Maza, J., Martin, P. G. & Angel, J. R. P., 1978. *Astrophys. J.*, **224**, 368.
Maza, J., 1979. *PhD dissertation*, University of Toronto.
McAlary, C. W., McLaren, R. A. & Crabtree, D. R., 1979. *Astrophys. J.*, **234**, 471.
Neugebauer, G., Becklin, E. E., Oke, J. B. & Searle, L., 1976. *Astrophys. J.*, **205**, 29.
Nilson, P., 1973. *Uppsala General Catalogue of Galaxies*, Uppsala.
Oke, J. B., 1974. *Astrophys. J. Suppl.*, **27**, 21.
Osterbrock, D. E., 1977. *Astrophys. J.*, **215**, 733.
Osterbrock, D. E., 1978. *Proc. Natn Acad. Sci. USA*, **75**, 540.
Penston, M. J., Penston, M. V. & Sandage, A., 1971. *Publs astr. Soc. Pacif.*, **83**, 783.
Poeckert, R., 1975. *Astrophys. J.*, **215**, 733.
Rieke, G. H., 1976. *Astrophys. J.*, **226**, 550.
Rieke, G. H., Lebofsky, M. J., Kemp, J. C., Coyne, G. V. & Tapia, S., 1977. *Astrophys. J.*, **218**, L37.
Rudnick, L., Owen, F. H., Jones, T. W., Puschell, J. J. & Stein, W. A., 1978. *Astrophys. J.*, **225**, L5.
Sanders, W. L., 1966. *Astr. J.*, **71**, 719.
Serkowski, K., 1973. *Astrophys. J.*, **179**, L101.
Serkowski, K., 1974. *Meth. exper. Phys.*, **12**, 361.
Serkowski, K., Mathewson, D. S. & Ford, V. L., 1975. *Astrophys. J.*, **196**, 261.
Shawl, S. J., 1975. *Astr. J.*, **80**, 595.
Stockman, H. S., Angel, J. R. P. & Beaver, E. A., 1976. *Bull. Am. astr. Soc.*, **8**, 45.
Stockman, H. S., 1979. Unpublished data.
Tapia, S., Craine, E. R., Gearhart, M. R., Pacht, E. & Kraus, J., 1977. *Astrophys. J.*, **215**, 71.
Thompson, I., Landstreet, J. D., Angel, J. R. P., Stockman, H. S., Woolf, N. J., Martin, P. G., Maza, J. & Beaver, E. A., 1979. *Astrophys. J.*, **229**, 909.
Visvanathan, N., 1973. *Astrophys. J.*, **179**, 1.
Wampler, E. J., 1971. *Astrophys. J.*, **164**, 1.
Weedman, D. W., 1973. *Astrophys. J.*, **183**, 29.
Weedman, D. W., 1978. *A. Rev. Astr. Astrophys.*, **15**, 69.
Woolf, N. J., Strittmatter, P. A., Rieke, G. H. & Beaver, E. A., 1976. *Bull. Am. astr. Soc.*, **8**, 290.